ISSN 2176-5480

22nd International Congress of Mechanical Engineering (COBEM 2013)
November 3-7, 2013, Ribeirão Preto, SP, Brazil

INFLUENCE OF CURVATURE VARIATIONS ON THE PRIMARY INSTABILITY DEVELOPMENT IN BOUNDARY LAYER FLOW

J K Rogenski
L F de Souza
Instituto de Ciências Matemáticas e de Computação, Universidade de São Paulo
josuelkr@gmail.com, lefraso@icmc.usp.br

J M Floryan
Western Engineering, University of Western Ontario
mfloryan@eng.uwo.ca

Abstract. *In the latter decades, numerical studies of the centrifugal instability have attracted interest of the scientific community due to their engineering applications. Since in practical situations the geometry of the problem is usually complex, the investigation of the effects of curvature variations is justified. The aim of this work is to investigate numerically how the curvature variations influence in the development of the primary instability. A Direct Numerical Simulation code written in vorticity-velocity formulation is used. The flow is decomposed into steady and perturbation parts. Periodicity in the spanwise direction is assumed in agreement with experimental observations. The time derivative is integrated using the classical fourth-order Runge-Kutta method. High-order, compact, finite-difference schemes are applied to discretize the spatial derivatives in the streamwise and wall normal directions. A spectral method is used to discretize the spatial derivatives in the spanwise direction. The Poisson equation is solved by a multigrid technique. The use of the Message Passing Interface library is adopted for code parallelization. The results are in agreement with predictions based on the Parabolized Stability Equation that are available in the literature. Convex curvature provides means for control of laminar flows as it modifies the inflectional spanwise and normal profiles of the streamwise velocity.*

Keywords: *Görtler vortices, curvature variations, turbulence transition, flow control*

1. INTRODUCTION

It is well known that imbalances between the radial pressure gradient and the centrifugal forces in a boundary layer may generate a secondary motion called Görtler instability. The Görtler flow distortions can produce strong secondary instability rising the flow to turbulence.

Experimental and numerical studies have been carried out aimed to better understanding of this phenomena. Classical experiments given by Swearigen and Blackwelder (1987) explicit the initial linear behavior of the Gortler vortices. In their studies both the mushroom-shaped structure and varicose and sinuose instabilities were observed in a flow over a wall with constant curvature.

However in practical situations the geometry of the problem is usually complex. As a consequence experimental investigations are difficult and numerical investigations become attractive alternatives.

Görtler vortices development over walls of variable curvature geometries was studied by Benmalek and Saric (1994). Their results explicit that convex regions has a stabilizing behavior over the growth of the vortices. This stable behavior is justified by Benmalek and Saric (1994) due to the tendency of the convex curvature in the elimination of inflectional streamwise velocity profile in the spanwise and wall-normal direction.

The present work provides Direct Numerical Simulation(DNS) results aimed to control the transition process by the use of variable curvature geometries.

2. FORMULATION

It is considered the motion of an incompressible, isothermal and Newtonian fluid flow on variable curvature geometries. The Navier-Stokes system of equation in vorticity–velocity formulation is used as alternative of the primitive variable one. Here vorticity is defined as the opposite of the curl of the velocity vector.

The same coordinate system presented by Floryan and Saric (1982) is used. The non-dimensional system of equation is expressed by

$$\frac{\partial \widetilde{\omega}_x}{\partial t} + \frac{\partial(\widetilde{\omega}_x\widetilde{v} - \widetilde{\omega}_y\widetilde{u})}{\partial y} - \frac{\partial(\widetilde{\omega}_z\widetilde{u} - \widetilde{\omega}_x\widetilde{w})}{\partial z} + \frac{Go^2}{\sqrt{Re}}\frac{\partial \widetilde{u}^2}{\partial z} = \frac{1}{Re}\nabla^2\widetilde{\omega}_x, \tag{1}$$

$$\frac{\partial \widetilde{\omega}_y}{\partial t} + \frac{\partial(\widetilde{\omega}_y\widetilde{w} - \widetilde{\omega}_z\widetilde{v})}{\partial z} - \frac{\partial(\widetilde{\omega}_x\widetilde{v} - \widetilde{\omega}_y\widetilde{u})}{\partial x} = \frac{1}{Re}\nabla^2\widetilde{\omega}_y, \tag{2}$$

ISSN 2176-5480

$$\frac{\partial\widetilde{\omega}_z}{\partial t}+\frac{\partial(\widetilde{\omega}_z\widetilde{u}-\widetilde{\omega}_x\widetilde{w})}{\partial x}-\frac{\partial(\widetilde{\omega}_y\widetilde{w}-\widetilde{\omega}_z\widetilde{v})}{\partial y}-\frac{Go^2}{\sqrt{Re}}\frac{\partial\widetilde{u}^2}{\partial x}=\frac{1}{Re}\nabla^2\widetilde{\omega}_z, \tag{3}$$

where $\widetilde{\omega}_x$, $\widetilde{\omega}_y$ and $\widetilde{\omega}_z$ are the vorticity components in stream(x), normal(y) and spanwise(z) directions respectively. $\widetilde{u}$, $\widetilde{v}$ e $\widetilde{w}$ are the velocity components in the x, y and z direction. The time is represented by the t variable.

The reference length is a characteristic plate length L and the reference velocity U_∞ is the free stream velocity. The Reynolds number is given by $Re=U_\infty L/\nu$, where ν is the kinematic viscosity. The Görtler number is given by $Go=Re^{0.25}\sqrt{R/L}$. The terms $Go^2\frac{\partial\widetilde{u}^2}{\partial x}/(\sqrt{Re})$ and $Go^2\frac{\partial\widetilde{u}^2}{\partial z}/(\sqrt{Re})$ are the curvature terms. R is the curvature radius.

The continuity equation is given by

$$\frac{\partial\widetilde{u}}{\partial x}+\frac{\partial\widetilde{v}}{\partial y}+\frac{\partial\widetilde{w}}{\partial z}=0. \tag{4}$$

Using the vorticity definition and the Eq. (4) one can obtain the following Poisson type equations:

$$\frac{\partial^2\widetilde{u}}{\partial x^2}+\frac{\partial^2\widetilde{u}}{\partial z^2}=-\frac{\partial\widetilde{\omega}_y}{\partial z}-\frac{\partial^2\widetilde{v}}{\partial x\partial y}, \tag{5}$$

$$\frac{\partial^2\widetilde{v}}{\partial x^2}+\frac{\partial^2\widetilde{v}}{\partial y^2}+\frac{\partial^2\widetilde{v}}{\partial z^2}=-\frac{\partial\widetilde{\omega}_z}{\partial x}+\frac{\partial\widetilde{\omega}_x}{\partial z}, \tag{6}$$

$$\frac{\partial^2\widetilde{w}}{\partial x^2}+\frac{\partial^2\widetilde{w}}{\partial z^2}=-\frac{\partial\widetilde{\omega}_y}{\partial x}-\frac{\partial^2\widetilde{v}}{\partial y\partial z}. \tag{7}$$

A perturbed formulation is applied, where a generic function $\widetilde{f}$ is rewritten as

$$\widetilde{f}=f_b+f, \tag{8}$$

where f_b is the base and f is the perturbation part of the function. $\widetilde{f}$ represent the global vorticity and velocity variables. Here the base flow is considered two-dimensional.

A system of equations is obtained by introducing Eq. (8) in Eq. (1)-(3) and (5)-(7), and then subtracting the base flow. Thus,

$$\frac{\partial\omega_x}{\partial t}+\frac{\partial a}{\partial y}-\frac{\partial b}{\partial z}+\frac{Go^2}{\sqrt{Re}}\frac{\partial d}{\partial z}=\frac{1}{Re}\nabla^2\omega_x, \tag{9}$$

$$\frac{\partial\omega_y}{\partial t}+\frac{\partial c}{\partial z}-\frac{\partial a}{\partial x}=\frac{1}{Re}\nabla^2\omega_y, \tag{10}$$

$$\frac{\partial\omega_z}{\partial t}+\frac{\partial b}{\partial x}-\frac{\partial c}{\partial y}-\frac{Go^2}{\sqrt{Re}}\frac{\partial d}{\partial x}=\frac{1}{Re}\nabla^2\omega_z, \tag{11}$$

$$\frac{\partial^2u}{\partial x^2}+\frac{\partial^2u}{\partial z^2}=-\frac{\partial\omega_y}{\partial z}-\frac{\partial^2v}{\partial x\partial y}, \tag{12}$$

$$\frac{\partial^2v}{\partial x^2}+\frac{\partial^2v}{\partial y^2}+\frac{\partial^2v}{\partial z^2}=-\frac{\partial\omega_z}{\partial x}+\frac{\partial\omega_x}{\partial z}, \tag{13}$$

$$\frac{\partial^2w}{\partial x^2}+\frac{\partial^2w}{\partial z^2}=\frac{\partial\omega_y}{\partial x}-\frac{\partial^2v}{\partial y\partial z}, \tag{14}$$

where the nonlinear terms a, b, c and d are:

$$a=\omega_x(v_b+v)-\omega_y(u_b+u), \tag{15}$$

$$b=(\omega_{z_b}+\omega_z)(u_b+u)-\omega_x w, \tag{16}$$

$$c=\omega_y w-(\omega_{z_b}+\omega_z)(v_b+v), \tag{17}$$

$$d=2u_bu+u^2. \tag{18}$$

Regarding the boundary conditions, at the upper boundary the flow was assumed to be irrotational. At the wall, the streamwise and normalwise velocity components are zero by the no-slip condition. At the outflow boundary the second derivative of the velocity and vorticity components are set to zero. Inflow boundary are specified based on a Blasius similar solution. The base flow is created by the use of the Blasius solution as an initial approximation (Schlichting, 1979).

ISSN 2176-5480

3. NUMERICAL METHOD

Justified by experimental evidences it is assumed periodicity in the spanwise direction. All the variables, in this sense, can be written as combination of K Fourier modes as follow

$$f(x,y,z,t) = \sum_{k=0}^{K} F_k(x,y,t)e^{-i\gamma_k z} \tag{19}$$

where f a variable, i is the imaginary unit , k is a Fourier mode and γ_k is the wave number in the spanwise direction. The wave number is defined as

$$\gamma_k = \frac{2\pi k}{\lambda_z},$$

where λ_z is the spanwise wave length of the fundamental Fourier mode.

The system of equation (9)-(14) is expressed (for each k Fourier mode) by:

$$\frac{\partial \Omega_{x_k}}{\partial t} + \frac{\partial A_k}{\partial y} + i\gamma_k B_k - \frac{Go^2}{\sqrt{Re}} i_k(D_k^2) = \frac{1}{Re}\nabla_k^2 \Omega_{x_k}, \tag{20}$$

$$\frac{\partial \Omega_{y_k}}{\partial t} - i\gamma_k C_k - \frac{\partial A_k}{\partial x} = \frac{1}{Re}\nabla_k^2 \Omega_{y_k}, \tag{21}$$

$$\frac{\partial \Omega_{z_k}}{\partial t} + \frac{\partial B_k}{\partial x} + \frac{\partial C_k}{\partial y} - \frac{Go^2}{\sqrt{Re}} \frac{\partial (D_k^2)}{\partial x} = \frac{1}{Re}\nabla_k^2 \Omega_{z_k}, \tag{22}$$

$$\frac{\partial^2 U_k}{\partial x^2} - {}^2_k U_k = i\gamma_k \Omega_{y_k} - \frac{\partial^2 V_k}{\partial x \partial y}, \tag{23}$$

$$\frac{\partial^2 V_k}{\partial x^2} + \frac{\partial^2 V_k}{\partial y^2} - \gamma_k^2 V_k = -\frac{\partial \Omega_{z_k}}{\partial x} - i\gamma_k \Omega_{x_k}, \tag{24}$$

$$\frac{\partial^2 W_k}{\partial x^2} - \gamma_k^2 W_k = \frac{\partial \Omega_{y_k}}{\partial x} + i\gamma_k \frac{\partial V_k}{\partial y}, \tag{25}$$

where $\nabla_k^2 = \left(\frac{\partial^2}{\partial x^2} + \frac{\partial^2}{\partial y^2} - \gamma_k^2\right)$.

The equations (20) to (25) are solved in a domain represent by Fig. 1.

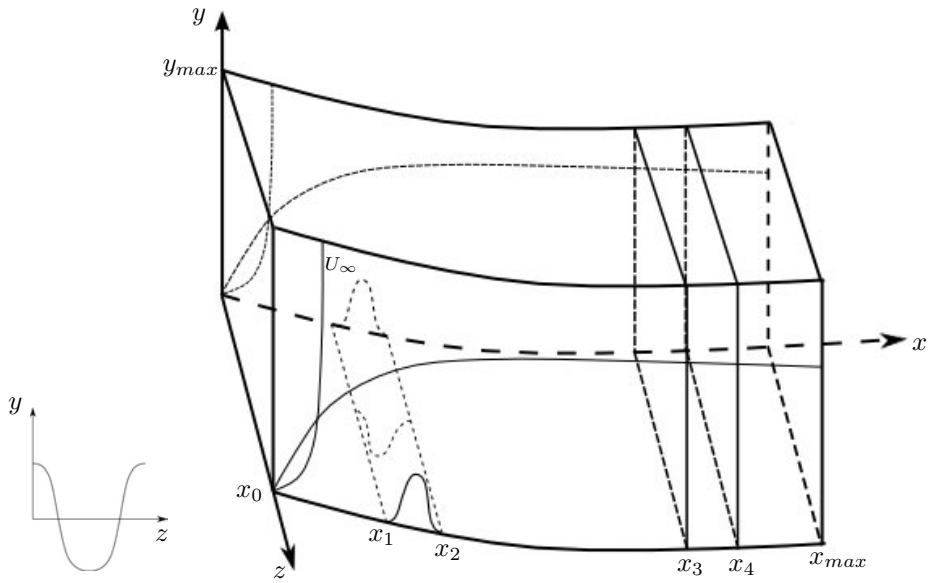

Figure 1: Physical domain

Calculations are performed in an orthogonal mesh parallel to the wall. A stretching technique is applied in the wall-normal direction. The fluid enters the computational domain at $x = x_0$ and exits at $x = x_{max}$. Disturbances are inserted in the domain by a mass suction/injection technique at the wall. The disturbance region is located between x_1 and x_2. In the region between x_3 and x_4 a buffer zone is adopted in order to avoid reflections (Kloker *et al.*, 1993). The baseflow solution uses boundary layers based on two-dimensional Navier-Stokes solution.

The temporal integration of the transport of vorticity equations are discretized by the use of a 4^a order Runge-Kutta method (Ferziger and Peric, 1997). Spatial derivatives are calculated using high order compact finite difference schemes

ISSN 2176-5480

(Souza *et al.*, 2005; Lele, 1992). The V–Poisson equation (24) – is solved by the use of a multigrid method called Full Approximation Scheme(FAS).

The large amount of points necessary to obtain acceptable results in a physical way justify the use of a parallel strategy. A domain decomposition strategy in the streamwise direction is adopted. The physical domain is partitioning into n equal parts. There is an overlap region and communications points are conveniently placed. The Message Passing Interface(MPI) library is used for the message-passing process.

4. THE CONCAVE-CONVEX CASE

Following Benmalek and Saric (1994) it is considered a wall distribution case given by

$$\kappa(x) = -\tanh\left[3\left(x-8\right)\right]\kappa_0 \tag{26}$$

where κ_0 is the curvature value at $x = 1$. This function is showed in Fig. 2 and can be interpreted as a concave circular arc attached to a convex one of same radius by a smooth curvature variation.

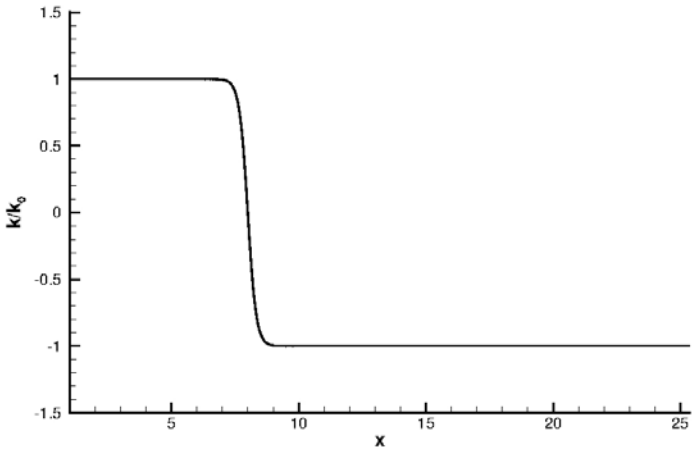

Figure 2: Wall curvature distribution - concave/convex case

It is important to notice that the convex region starts at the streamwise position $x = 8$ and at this position the vortices did not reach the saturation region.

Some linear simulations are carried out in order to find an acceptable range of disturbance amplitudes which represents Benmalek's test case. A linear simulation demands less computational time and its use can be justified due to the linear behavior of the Görtler modes close to the streamwise position $x = 8$.

Most parameters used for the numerical simulations agree with Swearigen and Blackwelder (1987) experimental data. It is used $L = 10^{-1}$ m and $U_\infty = 5$ m/s as length and velocity references. The Reynolds number is $Re = 33124$. The streamwise spatial step is 1.5×10^{-2}. The initial step in the normal direction is 5.0×10^{-4} and the stretching factor is 1%. The domain is discretized using 1625 points in the streamwise direction and 257 points in the normal flow direction. The wavenumber in the spanwise direction is given by $\gamma = 34.9066$. The disturbances are inserted between points 15 and 50 of the mesh in the x direction. The relaminarization zone is defined between the points 1515 and 1565. The time step is $dt = 7.8 \times 10^{-4}$.

Fig. 3 shows the energy of the second mode taking $A = 3.5 \times 10^{-3}, 5.0 \times 10^{-3}, 6.5 \times 10^{-3}$ and 1×10^{-2} as the maximum amplitude of the disturbance. The metric energy is defined (Lee and Liu, 1992; Li and Malik, 1995) as

$$E_k = \int_0^\infty \left(|U_k|^2 + |V_k|^2 + |W_k|^2\right) dy \text{ if k>0,} \tag{27}$$

and

$$E_k = \int_0^\infty \frac{1}{2}\left(|U_k|^2 + |W_k|^2\right) dy \text{ for k=0.} \tag{28}$$

Analyzing Fig. 3 a disturbance amplitude between 3.5×10^{-3} and 5.0×10^{-3} should be chosen. It is important to notice that the similar behavior of all the linear cases and the Benmalek and Saric (1994) result for the Fourier mode under investigation suggests no significant influence of nonlinearities. However a nonlinear numerical simulation is adopted and the maximum amplitude of disturbance is taken as 4×10^{-3}.

ISSN 2176-5480

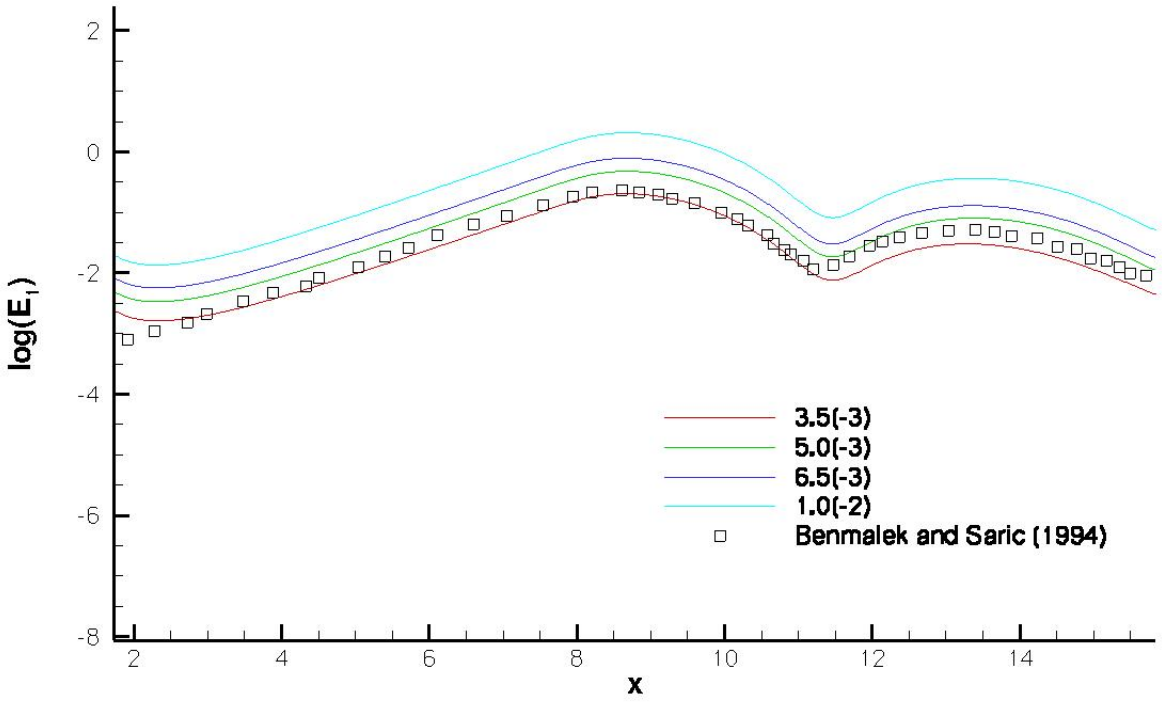

Figure 3: Second mode energy behavior (E_k) for different maximum disturbance amplitudes by linear simulations.

Nonlinear calculations are carried out using 32 physical points in the physical space and 11 Fourier modes in the Fourier space. The energy behavior in the streamwise direction of the modes 0 to 3 is present by Fig. 4

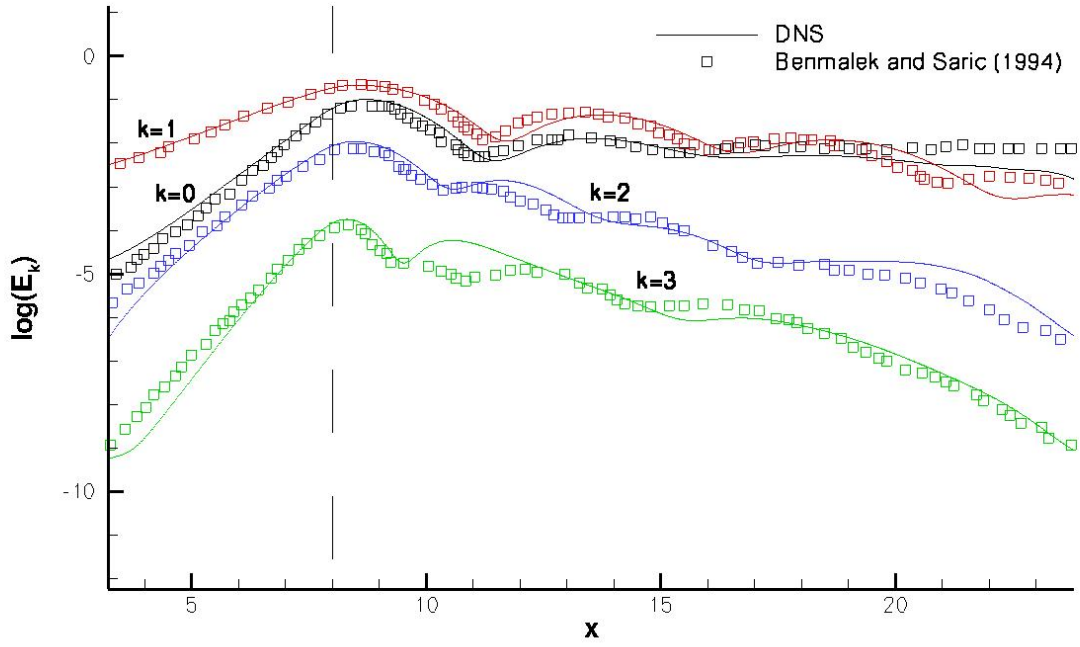

Figure 4: Energy behavior (E_k) of modes 0 to 3 - Concave/Convex curvature case

ISSN 2176-5480

Figure 4 explicits the influence of the convex curvature in terms of flow control. It is important to notice that there is a good agreement between the DNS simulation result and one presented by Benmalek and Saric (1994).

5. THE CONCAVE-ZERO CURVATURE CASE

In this case it is considered a wall distribution case given by

$$\kappa(x) = -0.5\left\{1 - \tanh\left[3\left(x - 10.24\right)\right]\right\}\kappa_0, \tag{29}$$

where κ_0 is the curvature value at $x = 1$. This function is showed in Fig. 5 and can be interpreted as a concave circular arc attached to a flat plate by a smooth curvature variation.

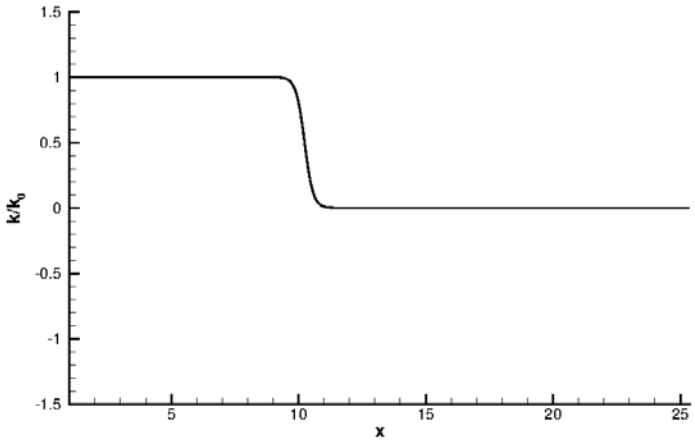

Figure 5: Wall curvature distribution - concave/zero curvature case

The flat region starts after $x = 10.24$ and at this position the vortices have already reached the saturation region. For this case the maximum amplitude of disturbances is taken $A = 7.0 \times 10^{-3}$.

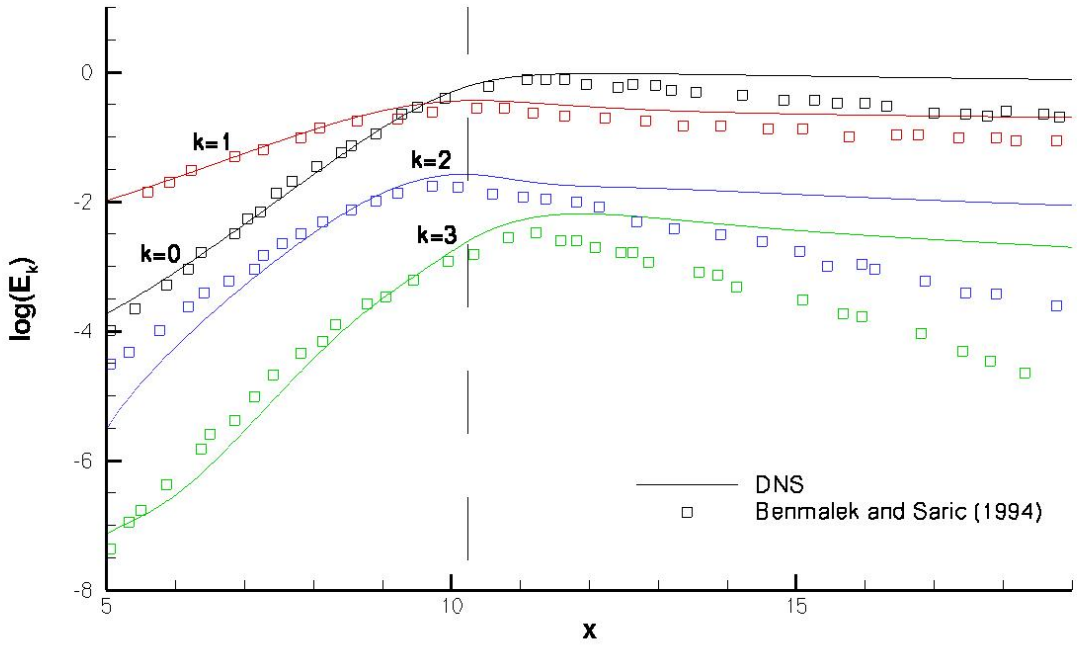

Figure 6: Energy behavior (E_k) of modes 0 to 3 - Concave/Zero curvature case

ISSN 2176-5480

Figure 6 explicits the influence of the zero curvature geometry. DNS result is different from the Benmalek and Saric (1994) after the curved wall region. The flat plate region provides some control over the flow but in a less effective way than results presented in literature since the energy of the modes decays slowly.

6. CONCLUSIONS

The use of Direct Numerical Simulation even demanding a high computation cost can be consider as a valuable strategy aimed to a better understating of the physical phenomena.

Specifically the use of this strategy to investigate the influence of curvature variation on flow control provides results that are in agreement with the literature. A convex curvature is able to suppress energy grows.

In the case of concave/flat plate simulation, the results did not agree with the presented results from Benmalek and Saric (1994). This differences can be explained by the simplifications in the governing equations to obtain the Parabolized Stability Equations, and also by the order of the approximation adopted by them.

7. ACKNOWLEDGEMENTS

Josuel thanks FAPESP for sponsorship under 2011/08010-0 and 2013/00553-0 processes and CAPES under DS-6713329/D process.

8. REFERENCES

Benmalek, A. and Saric, W.S., 1994. "Effects of curvature variation on the nonlinear evolution of Goertler vortices". *Physics of Fluids*, Vol. 6, pp. 3353–3367.

Ferziger, H. and Peric, M., 1997. *Computational methods for Fluid Dynamics*. Springer-Verlag, New York.

Floryan, M.J. and Saric, W.S., 1982. "Stability of Görtler vortices in boundary layers". *AIAA J.*, Vol. 20, pp. 316–324.

Kloker, M., Konzelmann, U. and Fasel, H.F., 1993. "Outflow boundary conditions for spatial Navier-Stokes simulations of transition boundary layers". *AIAA Journal*, Vol. 31, pp. 620–628.

Lee, K. and Liu, J.T.C., 1992. "On the growth of the mushroomline structures in nonlinear spatially developing goertler vortex flows". *Physics of Fluids*, Vol. A, pp. 1845–1847.

Lele, S., 1992. "Compact finite difference schemes with spectral-like resolution". *Journal Computations Physics*, Vol. 103, pp. 16–42.

Li, F. and Malik, M.R., 1995. "Fundamental and subharmonic secondary instabilities of görtler vortices". *J Fluid Mech.*, Vol. 295, pp. 77–100.

Schlichting, H., 1979. *Boundary Layer Theory*. John Wiley & Sons, McGraw-Hill, 7th edition.

Souza, L.F., Mendonca, M.T. and Medeiros, M.A.F., 2005. "The advantages of using high-order finite differences schemes in laminar–turbulent transition studies". *International Journal for Numerical Methods in Fluids*, Vol. 48, pp. 565–592.

Swearigen, J.D. and Blackwelder, R.F., 1987. "The growth and breakdown of streamwise vortices in the presence of a wall". *Journal of Fluid Mechanics*, Vol. 182, pp. 255–290.

9. RESPONSIBILITY NOTICE

The authors are the only responsible for the printed material included in this paper.